The effect of nonvertical shear on turbulence in a stably stratified medium

Frank G. Jacobitz and Sutanu Sarkar

Citation: Physics of Fluids (1994-present) **10**, 1158 (1998); doi: 10.1063/1.869640
View online: http://dx.doi.org/10.1063/1.869640
View Table of Contents: http://scitation.aip.org/content/aip/journal/pof2/10/5?ver=pdfcov
Published by the AIP Publishing

The effect of nonvertical shear on turbulence in a stably stratified medium

Frank G. Jacobitz and Sutanu Sarkar
Department of Applied Mechanics and Engineering Sciences, University of California, San Diego, La Jolla, California 92093-0411

(Received 2 January 1997; accepted 5 January 1998)

Direct numerical simulations were performed in order to investigate the evolution of turbulence in a stably stratified fluid forced by nonvertical shear. Past research has been focused on vertical shear flow, and the present work is the first systematic study with vertical and horizontal components of shear. The primary objective of this work was to study the effects of a variation of the angle θ between the direction of stratification and the gradient of the mean streamwise velocity from $\theta=0$, corresponding to the well-studied case of purely vertical shear, to $\theta=\pi/2$, corresponding to purely horizontal shear. It was observed that the turbulent kinetic energy K evolves approximately exponentially after an initial phase. The exponential growth rate γ of the turbulent kinetic energy K was found to increase nonlinearly, with a strong increase for small deviations from the vertical, when the inclination angle θ was increased. The increased growth rate is due to a strongly increased turbulence production caused by the horizontal component of the shear. The sensitivity of the flow to the shear inclination angle θ was observed for both low and high values of the gradient Richardson number Ri, which is based on the magnitude of the shear rate. The effect of a variation of the inclination angle θ on the turbulence evolution was compared with the effect of a variation of the gradient Richardson number Ri in the case of purely vertical shear. An effective Richardson number $\mathrm{Ri}_{\mathrm{eff}}$ was introduced in order to parametrize the dependence of the turbulence evolution on the inclination angle θ with a simple model based on mean quantities only. It was observed that the flux Richardson number Ri_f depends on the gradient Richardson number Ri but not on the inclination angle θ. © *1998 American Institute of Physics.* [S1070-6631(98)00905-2]

I. INTRODUCTION

Stably stratified shear flow is an ubiquitous feature of fluid motion in the geophysical environment. Consequently much attention has been drawn to the turbulence evolution in vertically stably stratified and vertically sheared flow motivated by oceanic and atmospheric applications.[1,2] The importance of the gradient Richardson number $\mathrm{Ri}=N^2/S^2$, where N is the Brunt–Väisälä frequency, and S is the shear rate, was discovered early by energy arguments.[1,3] The application of linear inviscid stability theory by Miles[4] and Howard[5] established $\mathrm{Ri}>1/4$ as the sufficient condition for stability in a stratified shear flow. More recently, laboratory experiments and direct numerical simulations have been performed in order to study many aspects of the turbulence evolution in vertically stratified and vertically sheared flow. The evolution of turbulence in vertically stably stratified and *nonvertically* sheared flow has received considerably less attention. The present paper appears to be the first systematic study of nonvertical shear flow.

A number of laboratory experiments on vertically stratified and vertically sheared flow have been performed. Komori *et al.*[6] investigated the turbulence structure in a stratified open-channel flow. Experiments on the evolution of homogeneous turbulence in stratified shear flow were performed by Rohr *et al.*[7] using a salt-stratified water channel, and by Piccirillo and Van Atta[8] using a thermally stratified wind tunnel. Itsweire *et al.* confirmed the importance of the gradient Richardson number Ri and Piccirillo and Van Atta addressed the Reynolds number dependence of the turbulence evolution. The experimental investigations were complemented by direct numerical simulations by Gerz *et al.*,[9] Holt *et al.*,[10] and Jacobitz *et al.*[11] In these simulations, the dependence of the turbulence evolution on a wide range of parameters was addressed. Gerz *et al.* studied the occurrence of counter gradient buoyancy fluxes at high Richardson numbers. Holt *et al.* addressed the Reynolds number dependence of the turbulence evolution. Jacobitz *et al.* investigated the possibility of Reynolds number independence at high Reynolds numbers and the influence of the shear number SK/ϵ, which is the ratio of a time scale of turbulence K/ϵ to the time scale imposed by the shear $1/S$. Here K is the turbulent kinetic energy and ϵ the turbulence dissipation rate. Kaltenbach *et al.*[12] performed large eddy simulations of vertically stratified and vertically sheared flow. In addition, passive scalars with linear gradients in all directions were introduced. It was observed that these scalars mix more efficiently in the horizontal than in the vertical.

Work on nonvertically sheared flow in a vertically stably stratified fluid is restricted to Blumen's[13] application of Howard's semicircle theorem to such a flow. Nonvertical shear flow in a stratified fluid occurs and has been studied indirectly in experimental investigations of wakes[14,15] and jets[16] in a stratified medium. No previous laboratory experiments or numerical investigations of the evolution of homogeneous turbulence in a nonvertical shear flow with vertical stratification are known to the authors. This is surprising as

this type of flow occurs frequently in environmental and engineering applications. Examples are flow over topography, river inflow into the ocean, or effluent discharge by power plants. The absence of previous work together with the wide range of applications are the primary motivation for the current study.

In vertical shear flow, the gradient Richardson number is usually defined with the vertical shear rate. In the case of more complex shear flows with additional nonvertical shear components, the definition of Ri may need to be modified. In nonvertical shear flow, we choose to define the gradient Richardson number as $\mathrm{Ri}=N^2/S^2$, where S is the magnitude of the shear rate. This selection is motivated by the observation that N is an external frequency scale imposed by the gravity acceleration and the mean stratification, while S is a distortion scale imposed by the mean velocity gradients. Therefore, the Richardson number $\mathrm{Ri}=N^2/S^2$, the square of the ratio of the two time scales, is a measure for the competing effects of mean stratification and mean shear.

In Sec. II the equations of motion are presented. In Sec. III the transport equations for second-order moments are discussed. The numerical method is summarized in Sec. IV. The results of direct numerical simulations are presented in Sec. V, and in Sec. VI the effective Richardson number is introduced. In Sec. VII the influence of additional parameters on the turbulence evolution is discussed. Section VIII contains a summary of the work presented here.

II. EQUATIONS OF MOTION

This study is based on the continuity equation of an incompressible fluid, the three-dimensional unsteady Navier–Stokes equation in the Boussinesq approximation, and a transport equation for the density. In the following, x_i denotes the ith component of an orthonormal Cartesian coordinate system, U_i the ith component of the total velocity, ϱ the total density, and P the total pressure. The dependent variables U_i, ϱ, and P are decomposed into a mean part (denoted by an overbar) and a fluctuating part (denoted by small letters):

$$U_i=\overline{U_i}+u_i, \quad \varrho=\overline{\varrho}+\rho, \quad P=\overline{P}+p. \tag{1}$$

The mean streamwise velocity $\overline{U}=(\overline{U_1},0,0)$ is unidirectional and has constant horizontal and vertical shear rates $\partial\overline{U_1}/\partial x_2=S_2=S\sin\theta$ and $\partial\overline{U_1}/\partial x_3=S_3=S\cos\theta$, respectively. The mean density has a constant vertical stratification rate $\partial\overline{\varrho}/\partial x_3=S_\rho$. Thus,

$$\overline{U_i}=(S\sin\theta x_2+S\cos\theta x_3)\delta_{i1}, \quad \overline{\varrho}=\rho_0+S_\rho x_3. \tag{2}$$

Therefore $\theta=0$ corresponds to the well-studied case of purely vertical shear shown in Fig. 1, and $\theta=\pi/2$ corresponds to the case of purely horizontal shear shown in Fig. 2. It is assumed that a mean pressure gradient balances the mean buoyancy force:

$$0=-\frac{\partial\overline{P}}{\partial x_3}-g(\rho_0+S_\rho x_3). \tag{3}$$

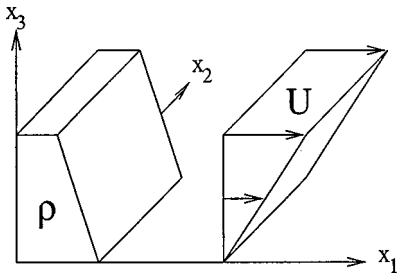

FIG. 1. Sketch of the mean velocity with vertical shear and the mean density with vertical stratification. This case corresponds to $\theta=0$.

The decomposition of the dependent variables is introduced into the equations of motion, and the following evolution equations for the fluctuating parts are obtained:

$$\frac{\partial u_j}{\partial x_j}=0, \tag{4}$$

$$\frac{\partial u_i}{\partial t}+u_j\frac{\partial u_i}{\partial x_j}+(S\sin\theta x_2+S\cos\theta x_3)\frac{\partial u_i}{\partial x_1}+(S\sin\theta u_2+S\cos\theta u_3)\delta_{i1}=-\frac{1}{\rho_0}\frac{\partial p}{\partial x_i}+\nu\frac{\partial^2 u_i}{\partial x_j\partial x_j}-\frac{g}{\rho_0}\rho\delta_{i3}, \tag{5}$$

$$\frac{\partial\rho}{\partial t}+u_j\frac{\partial\rho}{\partial x_j}+(S\sin\theta x_2+S\cos\theta x_3)\frac{\partial\rho}{\partial x_1}+S_\rho u_3=\alpha\frac{\partial^2\rho}{\partial x_j\partial x_j}. \tag{6}$$

Here g is the gravity acceleration, ν the kinematic viscosity, and α the scalar diffusivity.

III. TRANSPORT EQUATIONS

In this section the transport equations for second-order moments are introduced. The overbar $\overline{a}$ denotes the volume average of a. The transport equation for the velocity correlation $R_{ij}=\overline{u_iu_j}$ is derived from Eq. (5),

$$\frac{d}{dt}R_{ij}=P_{ij}-B_{ij}+\Pi_{ij}-\epsilon_{ij}, \tag{7}$$

$$P_{ij}=-S\sin\theta\overline{u_ju_2}\delta_{i1}-S\cos\theta\overline{u_ju_3}\delta_{i1}-S\sin\theta\overline{u_iu_2}\delta_{j1}-S\cos\theta\overline{u_iu_3}\delta_{j1}, \tag{8}$$

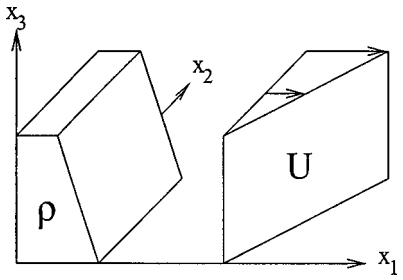

FIG. 2. Sketch of the mean velocity with horizontal shear and the mean density with vertical stratification. This case corresponds to $\theta=\pi/2$.

$$B_{ij}=\frac{g}{\rho_0}\,(\overline{u_i\rho}\,\delta_{j3}+\overline{u_j\rho}\,\delta_{i3}), \tag{9}$$

$$\Pi_{ij}=\frac{1}{\rho_0}\,\overline{p\left(\frac{\partial u_i}{\partial x_j}+\frac{\partial u_j}{\partial x_i}\right)}, \tag{10}$$

$$\epsilon_{ij}=2\nu\,\overline{\frac{\partial u_i}{\partial x_k}\frac{\partial u_j}{\partial x_k}}. \tag{11}$$

Here P_{ij} denotes the turbulence production term, B_{ij} the buoyancy term, Π_{ij} the pressure–strain term, and ϵ_{ij} the turbulence dissipation term. Note that the turbulence production term appears only in equations for velocity correlations that contain the streamwise velocity component, and that the buoyancy term appears only in equations for velocity correlations that contain the vertical velocity component. The equations for the components of the velocity correlation tensor are:

$$\frac{d}{dt}\,\overline{u_1u_1}=-2S\,\sin\,\theta\overline{u_1u_2}-2S\,\cos\,\theta\overline{u_1u_3}+\Pi_{11}-\epsilon_{11}, \tag{12}$$

$$\frac{d}{dt}\,\overline{u_2u_2}=\Pi_{22}-\epsilon_{22}, \tag{13}$$

$$\frac{d}{dt}\,\overline{u_3u_3}=-2\,\frac{g}{\rho_0}\,\overline{u_3\rho}+\Pi_{33}-\epsilon_{33}, \tag{14}$$

$$\frac{d}{dt}\,\overline{u_1u_2}=-S\,\sin\,\theta\overline{u_2u_2}-S\,\cos\,\theta\overline{u_2u_3}+\Pi_{12}-\epsilon_{12}, \tag{15}$$

$$\frac{d}{dt}\,\overline{u_1u_3}=-S\,\sin\,\theta\overline{u_2u_3}-S\,\cos\,\theta\overline{u_3u_3}-\frac{g}{\rho_0}\,\overline{u_1\rho}+\Pi_{13}-\epsilon_{13}, \tag{16}$$

$$\frac{d}{dt}\,\overline{u_2u_3}=-\frac{g}{\rho_0}\,\overline{u_2\rho}+\Pi_{23}-\epsilon_{23}. \tag{17}$$

The transport equations for the density fluxes $\overline{u_i\rho}$ are derived from Eqs. (5) and (6):

$$\frac{d}{dt}\,\overline{u_i\rho}=-S\,\sin\,\theta\overline{u_2\rho}\,\delta_{i1}-S\,\cos\,\theta\overline{u_3\rho}\,\delta_{i1}-S_\rho\overline{u_iu_3}-\frac{g}{\rho_0}\,\overline{\rho\rho}\,\delta_{i3}+\frac{1}{\rho_0}\,\overline{p\,\frac{\partial\rho}{\partial x_i}}-\frac{1+\mathrm{Pr}}{\mathrm{Pr}}\,\nu\,\overline{\frac{\partial\rho}{\partial x_k}\frac{\partial u_i}{\partial x_k}}. \tag{18}$$

The components of the above equation are:

$$\frac{d}{dt}\,\overline{u_1\rho}=-S\,\sin\,\theta\overline{u_2\rho}-S\,\cos\,\theta\overline{u_3\rho}-S_\rho\overline{u_1u_3}+\frac{1}{\rho_0}\,\overline{p\,\frac{\partial\rho}{\partial x_1}}-\frac{1+\mathrm{Pr}}{\mathrm{Pr}}\,\nu\,\overline{\frac{\partial\rho}{\partial x_k}\frac{\partial u_1}{\partial x_k}}, \tag{19}$$

$$\frac{d}{dt}\,\overline{u_2\rho}=-S_\rho\overline{u_2u_3}+\frac{1}{\rho_0}\,\overline{p\,\frac{\partial\rho}{\partial x_2}}-\frac{1+\mathrm{Pr}}{\mathrm{Pr}}\,\nu\,\overline{\frac{\partial\rho}{\partial x_k}\frac{\partial u_2}{\partial x_k}}, \tag{20}$$

$$\frac{d}{dt}\,\overline{u_3\rho}=-S_\rho\overline{u_3u_3}-\frac{g}{\rho_0}\,\overline{\rho\rho}+\frac{1}{\rho_0}\,\overline{p\,\frac{\partial\rho}{\partial x_3}}-\frac{1+\mathrm{Pr}}{\mathrm{Pr}}\,\nu\,\overline{\frac{\partial\rho}{\partial x_k}\frac{\partial u_3}{\partial x_k}}. \tag{21}$$

Finally a transport equation for the density fluctuations can by derived from Eq. (6):

$$\frac{d}{dt}\,\overline{\rho\rho}=-2S_\rho\overline{\rho u_3}-2\alpha\,\overline{\frac{\partial\rho}{\partial x_k}\frac{\partial\rho}{\partial x_k}}. \tag{22}$$

The transport equation for the turbulent kinetic energy $K=\overline{u_iu_i}/2$ is:

$$\frac{d}{dt}\,K=P_2+P_3-B-\epsilon, \tag{23}$$

$$P_2=-S\,\sin\,\theta\overline{u_1u_2}, \tag{24}$$

$$P_3=-S\,\cos\,\theta\overline{u_1u_3}, \tag{25}$$

$$B=\frac{g}{\rho_0}\,\overline{u_3\rho}, \tag{26}$$

$$\epsilon=\nu\,\overline{\frac{\partial u_i}{\partial x_k}\frac{\partial u_i}{\partial x_k}}. \tag{27}$$

Here P_2 is the turbulence production term due to horizontal shear $\partial U_1/\partial x_2$, P_3 the turbulence production term due to vertical shear $\partial U_1/\partial x_3$, B the buoyancy term, and ϵ the dissipation term. The total turbulence production is given by $P=P_2+P_3$. The potential energy K_ρ is computed from the density fluctuations:

$$K_\rho=\frac{1}{2}\,\frac{g}{\rho_0|S_\rho|}\,\overline{\rho\rho}. \tag{28}$$

IV. NUMERICAL APPROACH

The equations of motion are solved using a direct numerical approach. All dynamically important scales of the velocity and density fields are fully resolved. A method of lines approach is used where a spatial discretization is first performed in order to obtain a semidiscrete system of ordinary differential equations. Then the system of equations is integrated to advance the solution in time. The spatial discretization is accomplished by a Fourier collocation method, which yields high accuracy but can be used only for problems with periodic boundary conditions. Following a method originally used by Rogallo,[17] the equations of motion are transformed into a frame of reference moving with the mean flow in order to allow periodic boundary conditions on the fluctuating parts of the dependent variables. The temporal advancement is accomplished by a low-storage, third-order Runge–Kutta scheme. The initial conditions are taken from a simulation of decaying isotropic turbulence and allow for large scale growth. A computational grid with 144^3 points was used for all simulations. The evolution of the largest and smallest turbulence scales was monitored to ensure a proper resolution of the simulations.

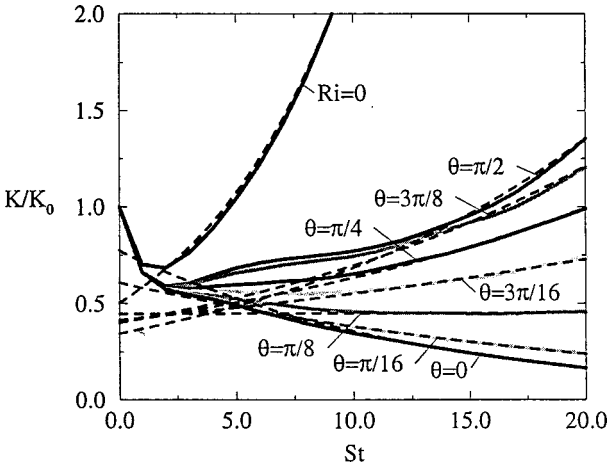

FIG. 3. Evolution of turbulent kinetic energy K as a function of the inclination angle θ. The dashed lines are the exponential approximation to the solution.

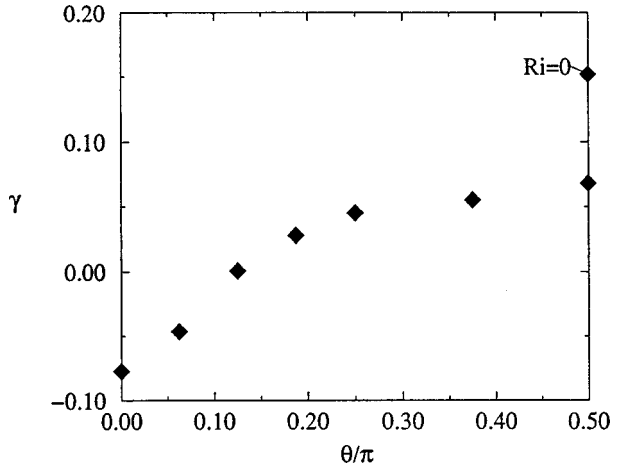

FIG. 4. Dependence of the asymptotic value of the growth rate γ on the inclination angle θ.

The code developed during our previous study of turbulence in a stratified fluid with vertical shear only ($\theta=0$) discussed in Jacobitz *et al.*[11] was modified to account for a variable shear inclination angle θ. The governing equations were written in a frame of reference (x_1',x_2',x_3') where x_1' is coincident with the x_1 direction. The x_2' and x_3' axes lie in the same plane as the x_2 and x_3 axes but are rotated around the x_1 axis by the inclination angle θ with respect to the x_2 and x_3 axes. The advantage of this new coordinate system is that there is a single mean shear component $S=\partial U_1'/\partial x_3'$, and the standard Rogallo transformation can be applied. In the new coordinate system, there are two gravity components $g_2'=g\sin\theta$ in the spanwise direction x_2' and $g_3'=g\cos\theta$ in the shear direction x_3' as well as two stratification components $S_\rho\sin\theta$ and $S_\rho\cos\theta$, respectively. However, the additional gravity and stratification components do not require any additional technique in the simulation.

V. RESULTS

In this section the results of a series of simulations with different shear inclination angles θ are presented. All simulations were started from the same initial conditions taken from a simulation of decaying isotropic turbulence without density fluctuations. The Richardson number $\mathrm{Ri}=N^2/S^2=0.2$ (where $N^2=-gS_\rho/\rho_0$ is the Brunt–Väisälä frequency), the Prandtl number $\mathrm{Pr}=\nu/\alpha=0.72$, the initial value of the Taylor microscale Reynolds number $\mathrm{Re}_\lambda=q\lambda/\nu=33.54$ (where $q=\sqrt{2K}$ is the magnitude of the velocity, and $\lambda=\sqrt{5\nu q^2/\epsilon}$ is the Taylor microscale), and the initial value of the shear number $SK/\epsilon=2.0$ are fixed. The Richardson number and the shear number are based on the magnitude $S=\sqrt{(dU_1/dx_2)^2+(dU_1/dx_3)^2}$ of the shear rates. While the Richardson number and the Prandtl number remain constant, the Reynolds number and the shear number evolve as the simulations are advanced in time.

Figure 3 shows the evolution of the turbulent kinetic energy K as a function of the nondimensional time St for different inclination angles θ. Initially K decays in all simulations due to the isotropic initial conditions. For $\theta=0$, which corresponds to the case of purely vertical shear shown in Fig. 1, the turbulent kinetic energy continues to decay throughout the simulation. In this case the stratification influences the shear production of turbulence directly. When the angle θ is increased, the decay of K is less strong. For $\theta=\pi/8$ the turbulent kinetic energy remains constant in time. For larger angles θ the evolution of the turbulent kinetic energy changes from decay to growth. For $\theta=\pi/2$, which corresponds to the case of purely horizontal shear shown in Fig. 2, the turbulent kinetic energy grows the strongest. However, the growth of K is not as strong as in the unstratified case (labeled $\mathrm{Ri}=0$ in Fig. 3) suggesting an indirect influence of the stratification on the turbulence production as discussed below.

In the case of purely vertical shear ($\theta=0$), the stratification influences the shear production directly. Buoyancy fluxes decrease the vertical velocity fluctuations $\overline{u_3u_3}$ [see Eq. (14)] and the magnitude of the 1–3 velocity correlation $\overline{u_1u_3}$ [see Eq. (16)]. Therefore the vertical shear production $P_3=-S\cos\theta\overline{u_1u_3}$ is directly reduced by buoyancy fluxes. It was shown in previous investigations[7,10,11] that the primary effect of stable stratification is to decrease the shear production and, to a smaller extent, act as a sink for turbulent kinetic energy through the buoyancy flux. In the case of purely horizontal shear ($\theta=\pi/2$), this direct mechanism of stabilization does not exist. The buoyancy fluxes still decrease the vertical velocity fluctuations and the 1–3 velocity correlation. However, there is no direct influence on the 1–2 velocity correlation $\overline{u_1u_2}$ [see Eq. (15)] and the horizontal shear production $P_2=-S\sin\theta\overline{u_1u_2}$. Only a redistribution through the pressure–strain terms leads to an indirect influence of stratification on the turbulence evolution in the case of purely horizontal shear.

It was found that the asymptotic evolution of the turbulent kinetic energy follows approximately an exponential law. In this case the exponential growth rate obtained from Eq. (23),

$$\gamma=\frac{1}{SK}\frac{dK}{dt}=\left(\frac{P_2}{SK}+\frac{P_3}{SK}-\frac{B}{SK}-\frac{\epsilon}{SK}\right), \tag{29}$$

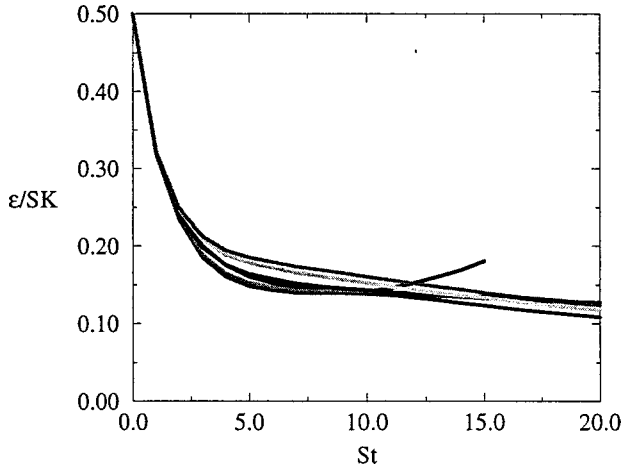

FIG. 5. Evolution of the normalized turbulence dissipation ϵ/SK as a function of the inclination angle θ.

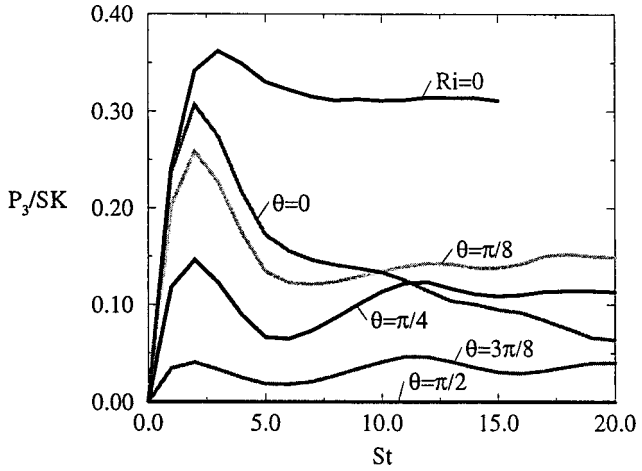

FIG. 7. Evolution of the normalized vertical turbulence production P_3/SK as a function of the inclination angle θ.

reaches an approximately constant value. Then the equation can be integrated and the exponential law

$$K = K_0 \exp(\gamma St) \tag{30}$$

is obtained. This exponential assumption is shown as dashed lines in Fig. 3. It approximates the asymptotic evolution well. The constant of integration is used to fit the graphs. The dependence of the asymptotic value of the growth rate γ on the inclination angle θ is shown in Fig. 4. The growth rate γ increases strongly for $0 \leqslant \theta \leqslant \pi/4$ and continues to increase mildly for $\pi/4 \leqslant \theta \leqslant \pi/2$. In the following, the dependence of each term on the right-hand side of Eq. (29) on the inclination angle θ is discussed.

Figure 5 shows the evolution of the normalized turbulence dissipation ϵ/SK. It appears that the normalized dissipation does not depend on the inclination angle θ. In Fig. 6, the evolution of the normalized buoyancy flux B/SK is shown. In the asymptotic regime, the normalized buoyancy flux increases with increasing angle θ. The asymptotic value of the normalized buoyancy flux is about twice as large in the case of purely horizontal shear ($\theta = \pi/2$) compared to the case of purely vertical shear ($\theta = 0$).

Figure 7 shows the evolution of the normalized turbulence production P_3/SK due to vertical shear. It vanishes for the case of purely horizontal shear ($\theta = \pi/2$) and increases as the inclination angle θ is decreased. The normalized vertical production P_3/SK decreases throughout the simulation of purely vertical shear ($\theta = 0$) due to the low Reynolds number of this strongly decaying case. The other cases reach an asymptotically approximately constant vertical production P_3/SK. Figure 8 shows the evolution of the normalized turbulence production P_2/SK due to horizontal shear. It vanishes for the case of purely vertical shear ($\theta = 0$), which includes the simulation of unstratified turbulence ($\mathrm{Ri} = 0$). As expected, P_2/SK increases as the angle θ is increased.

Due to the effect of buoyancy that exists at *all* shear inclination angles θ, the total normalized production rate P/SK (where $P = P_2 + P_3$) of the stratified cases is always smaller than the total normalized production rate of the unstratified case as shown in Fig. 9. Furthermore, since the effect of buoyancy acts directly in the vertical direction, the normalized turbulence production P/SK in the case of purely

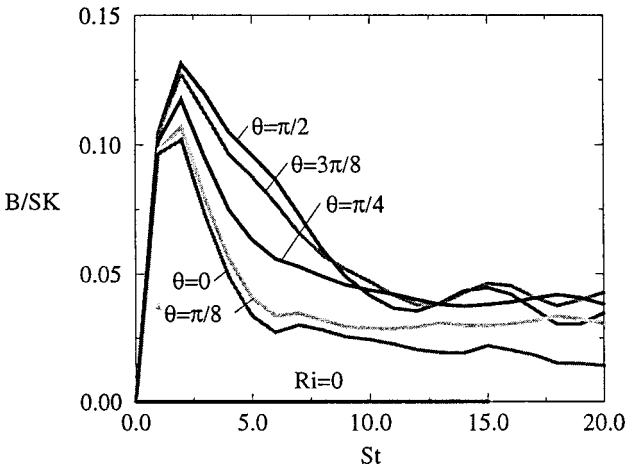

FIG. 6. Evolution of the normalized buoyancy flux B/SK as a function of the inclination angle θ.

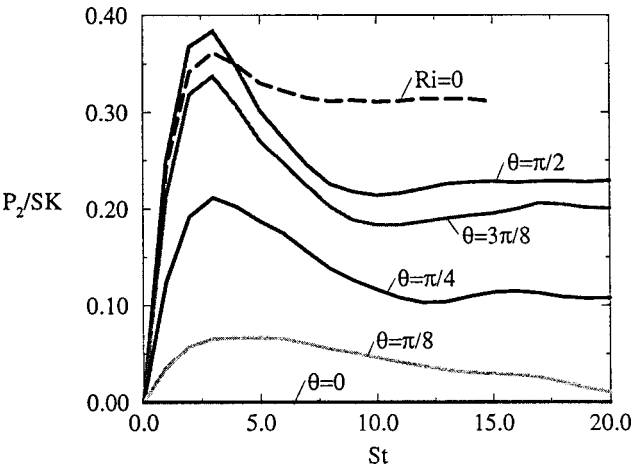

FIG. 8. Evolution of the normalized horizontal turbulence production P_2/SK as a function of the inclination angle θ.

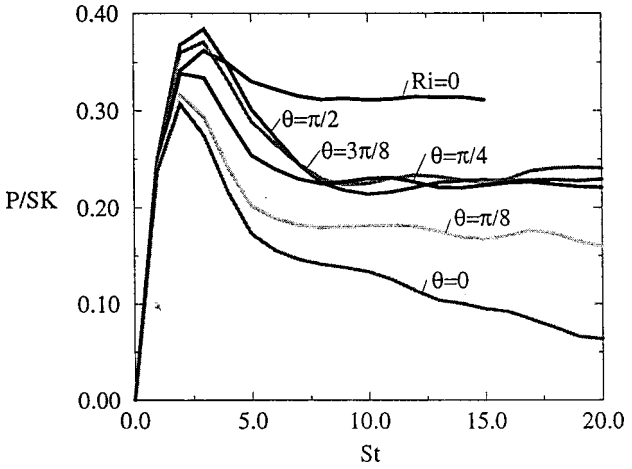

FIG. 9. Evolution of the normalized turbulence production P/SK as a function of the inclination angle θ.

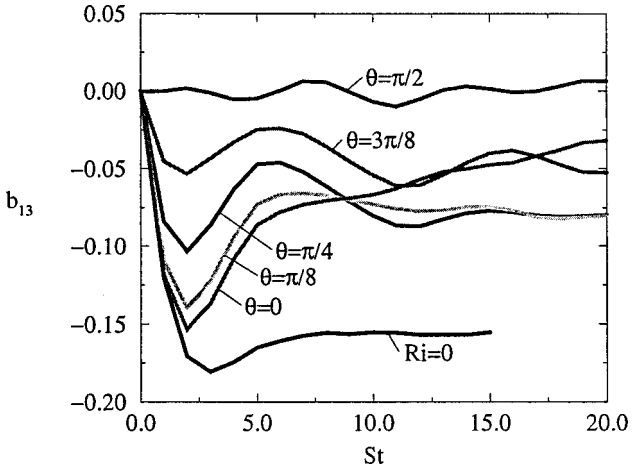

FIG. 10. Evolution of the Reynolds stress anisotropy b_{13} as a function of the inclination angle θ.

vertical shear is smaller than the normalized turbulence production in the case of purely horizontal shear.

The observation of a larger stabilizing effect of stable vertical stratification in the case of vertical shear relative to horizontal shear is consistent with the transport equations for the second-order moments. A buoyancy term appears directly in Eq. (14) for the vertical velocity variance $\overline{u_3u_3}$, reducing $\overline{u_3u_3}$. A buoyancy term also appears in Eq. (16) for the 1–3 velocity correlation $\overline{u_1u_3}$, and it reduces the magnitude of $\overline{u_1u_3}$ in addition to the reduction from $\overline{u_3u_3}$. The decreased $\overline{u_1u_3}$ reduces the vertical production rate $P_3 = -S \cos\theta \overline{u_1u_3}$. A similar direct influence of buoyancy on the horizontal production rate $P_2 = -S \sin\theta \overline{u_1u_2}$ does not exist, because a buoyancy term neither appears in Eq. (13) for $\overline{u_2u_2}$ nor in Eq. (15) for $\overline{u_1u_2}$. The 2–3 velocity correlation $\overline{u_2u_3}$ remains small compared to $\overline{u_1u_2}$ and $\overline{u_1u_3}$. However, there is an indirect effect of gravity through the pressure–strain terms on the horizontal turbulence production as shown in Fig. 8 by the reduced P_2/SK at $\theta = \pi/2$ with respect to the unstratified case.

The anisotropic action of buoyancy in the vertical direction is evident in the evolution of the Reynolds stress anisotropy tensor. In Fig. 10 the anisotropy b_{13} is shown, on which the normalized vertical production rate P_3/SK depends. The magnitude of the anisotropy b_{13} decreases with increasing angle θ. On the other hand, the magnitude of the anisotropy b_{12} increases with increasing angle θ as shown in Fig. 11. The anisotropy b_{12} determines the normalized horizontal production rate P_2.

VI. THE EFFECTIVE RICHARDSON NUMBER

In this section, the effective Richardson number $\mathrm{Ri}_{\mathrm{eff}}$ is introduced in order to parametrize the dependence of the turbulence evolution on the shear inclination angle θ. In addition, the relationship between the effective Richardson number $\mathrm{Ri}_{\mathrm{eff}}$, the flux Richardson number Ri_f, and the gradient Richardson number Ri is discussed.

A series of simulations with different gradient Richardson numbers Ri but purely vertical shear was performed. These simulations matched the initial conditions of the series of simulations with constant gradient Richardson numbers Ri but different inclination angles θ discussed in Sec. V. Again, an exponential evolution of the turbulent kinetic energy K was observed as shown in Fig. 12. The turbulent kinetic energy K decays for large Ri and grows for small Ri. The value of the critical Richardson number, for which K remains constant in time, is about $\mathrm{Ri}_{\mathrm{cr}} = 0.138$ in this series of simulations. The dependence of the asymptotic value of the growth rate γ on the gradient Richardson number Ri is shown in Fig. 13. In agreement with Jacobitz *et al.*[11] the growth rate γ decreases approximately linearly with increasing Richardson number Ri. The following relationship was obtained from linear regression:

$$\gamma = 0.156(6) - 1.13(4)\mathrm{Ri}. \tag{31}$$

In the oceanic and atmospheric environment, the flux Richardson number $\mathrm{Ri}_f = B/P$ is frequently used instead of the gradient Richardson number Ri. The flux Richardson number Ri_f can be related to the gradient Richardson number Ri, if an eddy diffusivity model is used:

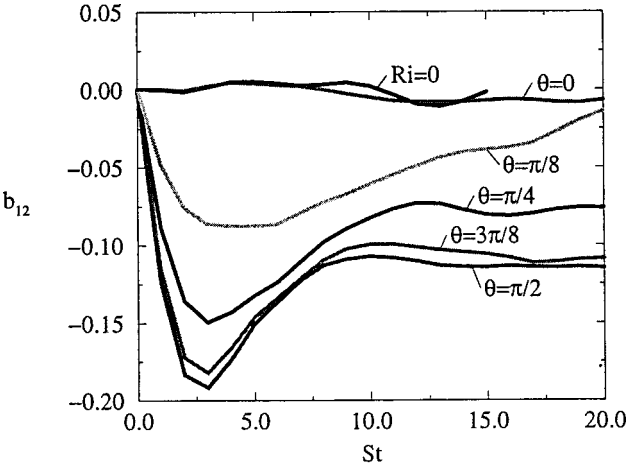

FIG. 11. Evolution of the Reynolds stress anisotropy b_{12} as a function of the inclination angle θ.

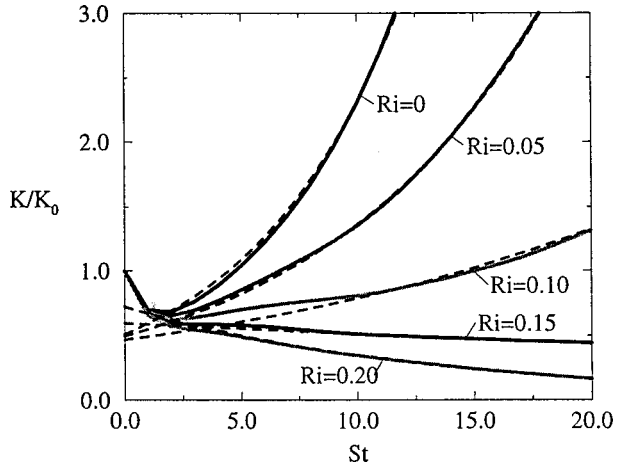

FIG. 12. Evolution of the turbulent kinetic energy K for different gradient Richardson numbers Ri in the case of purely vertical shear ($\theta=0$). The dashed lines are the exponential approximation to the solution.

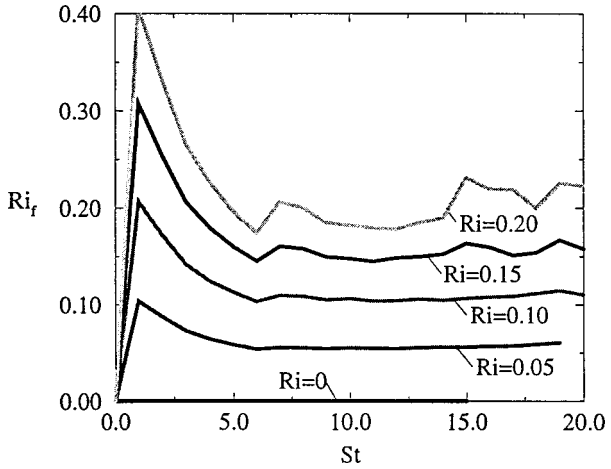

FIG. 14. Evolution of the flux Richardson number Ri_f for different gradient Richardson numbers Ri in the case of purely vertical shear ($\theta=0$).

$$\mathrm{Ri}_f=\frac{B}{P}=-\frac{g}{\rho_0}\frac{\overline{u_3\rho}}{S\overline{u_1'u_3'}}=-\frac{\alpha_t}{\nu_t}\frac{g}{\rho_0}\frac{S_\rho}{S^2}=\frac{\mathrm{Ri}}{\mathrm{Pr}_t}. \tag{32}$$

Here $u_1'=u_1$ and $u_3'=u_2\sin\theta+u_3\cos\theta$ are the velocity components in the plane of shear, $\alpha_t=-\overline{u_3\rho}/S_\rho$ is the eddy diffusivity of the density field, $\nu_t=-\overline{u_1'u_3'}/S$ is the eddy viscosity of the velocity field, and $\mathrm{Pr}_t=\nu_t/\alpha_t$ is the turbulent Prandtl number. Therefore the flux Richardson number Ri_f coincides with the gradient Richardson number Ri, if the turbulent Prandtl number Pr_t is equal to one.

The evolution of the flux Richardson number Ri_f is shown in Fig. 14 for different gradient Richardson numbers Ri in the case of purely vertical shear. For all gradient Richardson numbers Ri, the flux Richardson number Ri_f evolves to a constant asymptotic value that is close to the corresponding value of the gradient Richardson number Ri. Therefore, in the parameter range considered here, the turbulent Prandtl number Pr_t remains always close to one. This agrees with previous simulations by Schumann and Gerz[18] where an increase of the turbulent Prandtl number Pr_t with increasing Richardson number Ri is observed only at larger Richardson numbers $\mathrm{Ri}>0.25$, beyond the scope of the current work. Figure 15 shows the evolution of the flux Richardson number Ri_f for different inclination angles θ and constant gradient Richardson number $\mathrm{Ri}=0.2$. The asymptotic value of Ri_f remains very close to the value of $\mathrm{Ri}=0.2$. Therefore the turbulent Prandtl number Pr_t is again close to one.

In the case of nonvertical shear it was shown in Fig. 4 that the growth rate γ depends on the inclination angle θ for a constant gradient Richardson number Ri. Using the linear relationship (31) between the growth rate γ and the Richardson number Ri, an effective Richardson number $\mathrm{Ri}_{\mathrm{eff}}$ can be computed from the growth rates γ observed at an angle θ. Therefore the effective Richardson number $\mathrm{Ri}_{\mathrm{eff}}$ of a nonvertical shear flow is defined to be equal to the gradient Richardson number Ri of a purely vertical shear flow with the same growth rate γ. The dependence of the effective Richardson number $\mathrm{Ri}_{\mathrm{eff}}$ on the inclination angle θ is shown in Fig. 16. The effective Richardson number $\mathrm{Ri}_{\mathrm{eff}}$ decreases

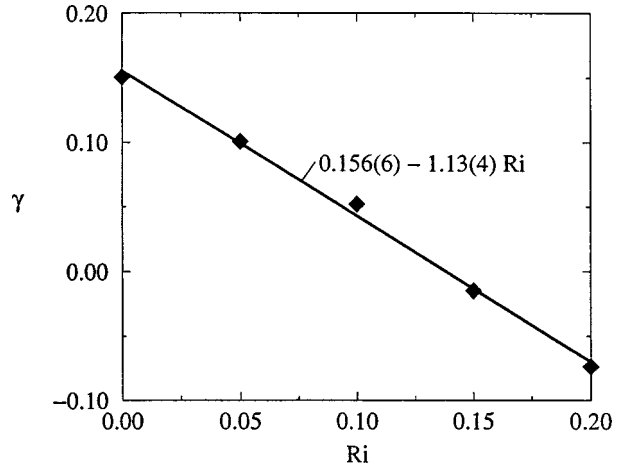

FIG. 13. Dependence of the asymptotic value of the growth rate γ on the gradient Richardson number Ri for the case of purely vertical shear ($\theta=0$).

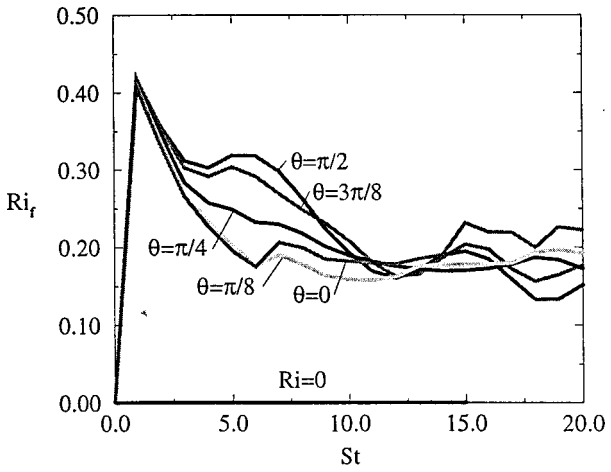

FIG. 15. Evolution of the flux Richardson number Ri_f for different inclination angles θ.

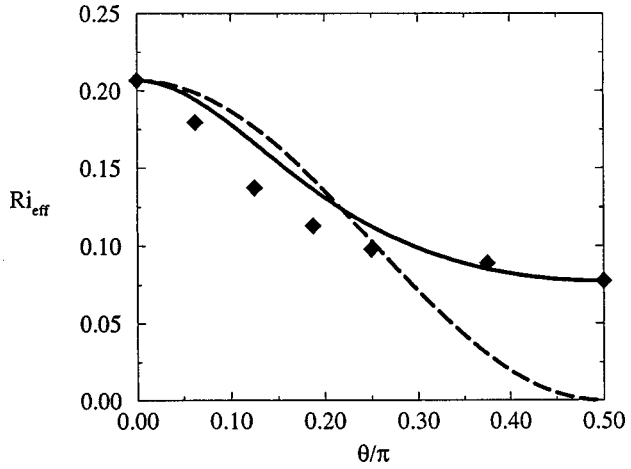

FIG. 16. Dependence of the effective Richardson number Ri_{eff} on the inclination angle θ. The diamonds represent the direct numerical results, the dashed line represents Eq. (33) and the solid line represents Eq. (34).

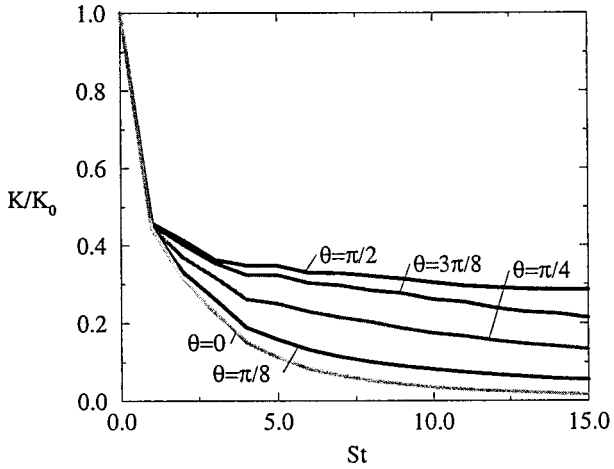

FIG. 17. Evolution of the turbulent kinetic energy K for different shear inclination angles θ in the case of strong stratification with Ri=2.0.

with increasing angle θ, because the stabilizing influence of stable stratification decreases as the shear inclination angle θ is increased from $\theta=0$ (vertical shear) to $\theta=\pi/2$ (horizontal shear). In the following paragraphs two possible models for the observed dependence are discussed.

First consider the plane of shear defined by the velocity components u_1 and $u_2 \sin\theta+u_3\cos\theta$. This plane is the (x_1',x_3') plane discussed in Sec. IV on the numerical approach. The mean shear S acts only in this plane. The components $g\cos\theta$ and $S_\rho\cos\theta$ of the gravity constant g and the stratification S_ρ act also in this plane. Under the assumption that the components $g\sin\theta$ and $S_\rho\sin\theta$ outside the plane of shear do not influence the evolution of turbulence, the effective Richardson number can be written as:

$$\mathrm{Ri}_{\mathrm{eff}}=\mathrm{Ri}\cos^2\theta. \tag{33}$$

This relation is shown as a dashed line in Fig. 16. It does not fit the numerical data well and leads to large errors at large values of the inclination angle θ, because it does not take the effect of buoyancy outside the plane of shear into account.

In a second approach, the shear $S\cos\theta$ in the direction of gravity and $S\sin\theta$ perpendicular to the direction of gravity are weighted differently. Since the horizontal component $S\sin\theta$ is not directly influenced by gravity, it is given a larger weight than the vertical component $S\cos\theta$. Then the effective Richardson number $\mathrm{Ri}_{\mathrm{eff}}$ can be written as:

$$\mathrm{Ri}_{\mathrm{eff}}=\frac{\mathrm{Ri}}{\cos^2\theta+a\sin^2\theta}. \tag{34}$$

Here $a=2.7$ is the weight given to the horizontal component of shear. Equation (34) is shown as a solid line in Fig. 16. It fits the numerical data relatively well for a simple model based on mean parameters of the flow.

VII. INFLUENCE OF ADDITIONAL PARAMETERS

The primary aim of this work was to study the influence of the shear inclination angle θ on the dynamics of turbulence in stratified shear flow, keeping other parameters constant. However, more simulations have been performed to study the influence of additional parameters. First, the persistence of the shear inclination angle effect in strongly stratified, high Richardson number flow is studied. Then the influence of a high initial shear number is discussed.

In the first series of simulations discussed in Sec. V, the shear inclination angle θ was varied from $\theta=0$ to $\theta=\pi/2$ to study the influence of the inclination angle on the turbulence evolution. All other parameters were fixed in these simulations. In the second series of simulations discussed in Sec. VI, the gradient Richardson number Ri was varied from Ri $=0$ to Ri$=0.2$ in order to compare its influence on the turbulence evolution in vertically stratified and vertically sheared flow with the effects of a variation of the inclination angle θ in vertically stratified and nonvertically sheared flow. Both parameters influence the growth rate γ of the turbulent kinetic energy K. Since stratification effects are often parametrized by the gradient Richardson number Ri, the shear inclination angle effect was parametrized by the introduction of the effective Richardson number $\mathrm{Ri}_{\mathrm{eff}}$. The second series of simulations covers only a limited range of Richardson numbers that result in growth rates similar to those observed in the first series of simulations.

An additional series of simulations performed to study the influence of the shear inclination angle on the turbulence evolution at a large gradient Richardson number is now discussed. The objective of these simulations is to confirm that the sensitivity to the inclination angle θ, as seen in the results presented in Sec. V with Ri$=0.2$, persists in a strongly stratified medium with Ri$=2.0$. All simulations were started from the same initial conditions with Ri$=2.0$, Pr$=0.72$, initial $\mathrm{Re}_\lambda=33.54$, and initial $SK/\epsilon=2.0$. Figure 17 shows the evolution of the turbulent kinetic energy K as a function of the nondimensional time St for different angles θ. For all cases the turbulent kinetic energy K decays due to the strong stable stratification. However, the growth rates γ vary for different angles θ. Figure 18 shows the dependence of the growth rate γ as a function of the angle θ for Ri$=2.0$ (open diamonds) and Ri$=0.2$ (filled diamonds). Both series show a qualitatively similar increase of the growth rate γ with increasing angle θ. In agreement with the Ri$=0.2$ case, the asymptotic

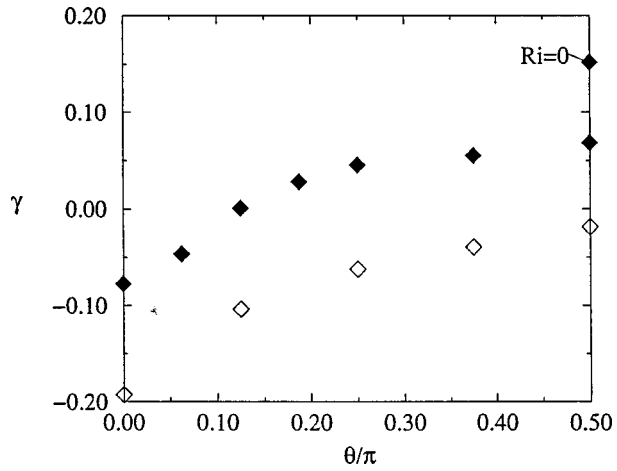

FIG. 18. Dependence of the growth rate γ on the shear inclination angle θ in the case Ri$=0.2$ (filled diamonds) and Ri$=2.0$ (open diamonds).

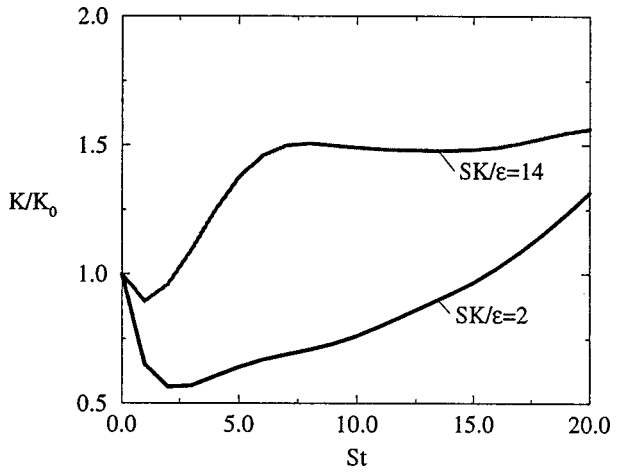

FIG. 20. Evolution of the turbulent kinetic energy K for different shear numbers SK/ϵ in the case of purely horizontal shear ($\theta=\pi/2$).

value of the flux Richardson number $\mathrm{Ri}_f=0.3-0.4$ was found to be relatively insensitive to the angle variation in the strongly stratified Ri$=2.0$ case. The large value of the turbulent Prandtl number $\mathrm{Pr}_t=5-7$ agrees with the results of Schumann and Gerz.[18]

Now consider only the case of purely horizontal shear ($\theta=\pi/2$). The Ri$=0.2$ case shows strong growth of K as discussed in Sec. V. The Ri$=2.0$ case, on the other hand, shows a slight decay of K. Therefore strong stable stratification is able to suppress the growth of K in the case of horizontal shear despite the absence of the direct mechanism that is responsible for the suppression of growth in the case of vertical shear. However, the value of the critical Richardson number Ri_{cr} at which growth is suppressed is about an order of magnitude larger in the case of horizontal shear compared to the case of vertical shear.

The shear number SK/ϵ has an important influence on the turbulence evolution in vertically sheared and stratified flow as discussed in Jacobitz *et al.*[11] Therefore additional simulations with high initial shear numbers were performed in purely vertical shear ($\theta=0$) and in purely horizontal shear ($\theta=\pi/2$) to ascertain if the shear number effect persists in the case of purely horizontal shear. Figure 19 shows the evolution of the turbulent kinetic energy K for different initial shear numbers in the case of vertical shear. The simulations were started from the same initial conditions with Ri$=0.1$, Pr$=0.72$, and $\mathrm{Re}_\lambda=33.54$. The turbulent kinetic energy K grows for the cases with initial $SK/\epsilon=2.0$ and $SK/\epsilon=6.0$ but decays for the case with initial $SK/\epsilon=14.0$. Figure 20 shows the evolution of K in the case of horizontal shear. The simulations were started with the same initial conditions with Ri$=0.2$, Pr$=0.72$, and $\mathrm{Re}_\lambda=33.54$. The turbulent kinetic energy grows strongly for $SK/\epsilon=2.0$ but grows only mildly for $SK/\epsilon=14.0$. Figure 21 shows the corresponding growth rates γ. The cases with high initial shear numbers finally result in an evolution with a smaller exponential growth rate than the corresponding cases with low initial shear numbers. Therefore the stabilizing effect of high shear number flow that was observed by Jacobitz *et al.*[11] in the case of vertical shear persists in the case of horizontal shear.

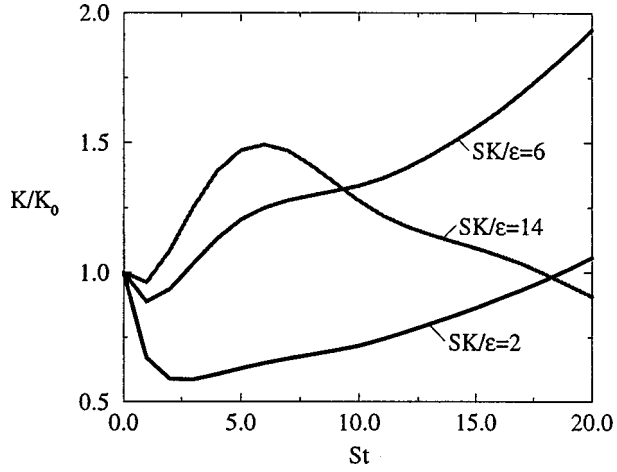

FIG. 19. Evolution of the turbulent kinetic energy K for different shear numbers SK/ϵ in the case of purely vertical shear ($\theta=0.0$).

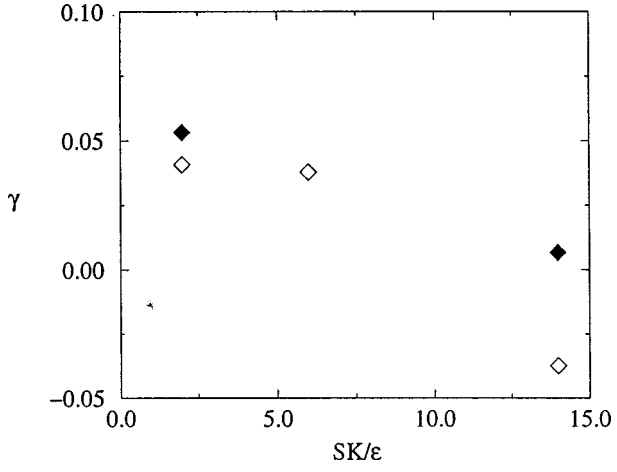

FIG. 21. Dependence of the growth rate γ on the initial value of the shear number SK/ϵ in the case of purely horizontal shear (filled diamonds) and purely vertical shear (open diamonds).

VIII. CONCLUSIONS

The effect of both vertical and horizontal shear components in a vertically stably stratified fluid has been investigated using direct numerical simulations. To the best of our knowledge, no such study, either experimental or numerical, has been performed previously. It was found that not only the magnitude of the shear but also its orientation relative to the vertical direction of gravity and stratification has a significant effect on the flow dynamics.

Two series of direct numerical simulations were initially performed. In the first series, the shear inclination angle θ between the direction of stratification and the gradient of the mean streamwise velocity was varied from $\theta=0$, corresponding to purely vertical shear, to $\theta=\pi/2$, corresponding to purely horizontal shear. The gradient Richardson number $\mathrm{Ri}=0.2$ based on the magnitude of the shear rate S was fixed. In the second series, the gradient Richardson number Ri was varied from $\mathrm{Ri}=0$, corresponding to unstratified shear flow, to $\mathrm{Ri}=0.2$. The angle $\theta=0$ was fixed in this simulation. All simulations were started from the same initial conditions taken from a simulation of decaying isotropic turbulence with no density fluctuations. The initial value of the Taylor microscale Reynolds number $\mathrm{Re}_\lambda=33.54$, the initial value of the shear number $SK/\epsilon=2.0$, and the Prandtl number $\mathrm{Pr}=0.72$ were fixed for all simulations.

The turbulent kinetic energy was found to evolve exponentially after an initial period of decay for all simulations. For the first series of simulations, the exponential growth rate γ was found to increase with the inclination angle θ as shown in Fig. 4. This increase is due to a strong increase of the horizontal turbulence production P_2 caused by the horizontal component of shear as θ is increased. Although the vertical turbulence production P_3 decreases when θ is increased, the net turbulence production $P=P_2+P_3$ increases. An examination of the transport equations for the second-order moments shows that there is a direct influence of the buoyancy on the vertical turbulence production but no direct influence on the horizontal turbulence production. Therefore the turbulence production in the case of purely horizontal shear is stronger than the turbulence production in the case of purely vertical shear, but due to the three-dimensional character of turbulence, the turbulence production in the case of purely horizontal shear is still smaller than the turbulence production in unstratified shear flow. Therefore the growth rate γ is smaller in the case of horizontal shear with respect to that in the unstratified case.

For the second series of simulations, the exponential growth rate γ was found to decrease approximately linearly with increasing gradient Richardson number Ri over the range $0\leqslant\mathrm{Ri}\leqslant0.2$ as shown in Fig. 13, in agreement with previous simulations.[11] In order to incorporate the effect of the shear inclination angle variation into a single parameter, the effective Richardson number $\mathrm{Ri}_{\mathrm{eff}}$ was introduced. The effective Richardson number $\mathrm{Ri}_{\mathrm{eff}}$ of a nonvertical shear flow is defined to be equal to the gradient Richardson number Ri of a purely vertical shear flow with the same growth rate γ. The effective Richardson number was found to decrease with increasing inclination angle θ as shown in Fig. 16. A simple model was used to capture the dependence of the effective Richardson number $\mathrm{Ri}_{\mathrm{eff}}$ on the angle θ. In this model the horizontal component of shear is weighted more strongly than the vertical component of shear, because the horizontal component of shear production is not directly influenced by buoyancy and therefore contributes more strongly to the net turbulence production than the vertical component of shear production.

It was also observed that, for the parameter range studied here, the flux Richardson number Ri_f depends on the gradient Richardson number Ri but not on the shear inclination angle θ. It is interesting that the normalized turbulence production is strongly influenced by the angle θ, but that the flux Richardson number remains unaffected.

An additional series of simulations was performed to study the influence of the shear inclination angle θ of the turbulence evolution in a strongly stratified medium with $\mathrm{Ri}=2.0$ It was found that the angle effect persists in high Richardson number flow. The value of the critical Richardson number $\mathrm{Ri}_{\mathrm{cr}}$, at which growth of the turbulent kinetic energy is suppressed, is about an order of magnitude larger in the case of horizontal shear compared with the case of vertical shear. The flux Richardson number Ri_f was again found to be relatively insensitive to the angle variation. Additional simulations confirmed that our earlier observation of the stabilizing effect of a large initial shear number SK/ϵ in vertically sheared flow applies in horizontally sheared flow too.

ACKNOWLEDGMENTS

The study of the turbulence evolution in a stably stratified fluid forced by horizontal shear was suggested by Charles W. Van Atta. The authors want to acknowledge his ongoing support of this work. This study is supported by the Office of Naval Research, Physical Oceanography Program, through Grant No. ONR N00014-94-1-0223. Supercomputer time was provided by the San Diego Supercomputer Center (SDSC) and the US Army Corps of Engineers Waterways Experiment Station (WES).

[1] L. F. Richardson, ''The supply of energy from and to atmospheric eddies,'' Proc. R. Soc. London, Ser. A **97**, 354 (1920).
[2] A. A. Townsend, ''Turbulent flow in a stably stratified atmosphere,'' J. Fluid Mech. **3**, 361 (1957).
[3] G. I. Taylor, Adams Prize Essay (unpublished, 1914).
[4] J. W. Miles, ''On the stability of heterogeneous shear flows,'' J. Fluid Mech. **10**, 496 (1961).
[5] L. N. Howard, Note on a paper of John W. Miles. J. Fluid Mech. **10**, 509 (1961).
[6] S. Komori, H. Ueda, F. Ogino, and T. Mizushina, ''Turbulence structure in stably stratified open-channel flow,'' J. Fluid Mech. **130**, 13 (1983).
[7] J. J. Rohr, E. C. Itsweire, K. N. Helland, and C. W. Van Atta, ''Growth and decay of turbulence in a stably stratified shear flow,'' J. Fluid Mech. **195**, 77 (1988).
[8] P. S. Piccirillo and C. W. Van Atta, ''The evolution of a uniformly sheared thermally stratified turbulent flow,'' J. Fluid Mech. **334**, 61 (1997).
[9] T. Gerz, U. Schumann, and S. E. Elghobashi, ''Direct numerical simulation of stratified homogeneous turbulent shear flows,'' J. Fluid Mech. **200**, 563 (1989).
[10] S. E. Holt, J. R. Koseff, and J. H. Ferziger, ''A numerical study of the evolution and structure of homogeneous stably stratified sheared turbulence,'' J. Fluid Mech. **237**, 499 (1992).
[11] F. G. Jacobitz, S. Sarkar, and C. W. Van Atta, ''Direct numerical simula-

tions of the turbulence evolution in a uniformly sheared and stably stratified flow,'' J. Fluid Mech. **342**, 231 (1997).
[12]H.-J. Kaltenbach, T. Gerz, and U. Schumann, ''Large-eddy simulation of homogeneous turbulence and diffusion in stably stratified shear flow,'' J. Fluid Mech. **280**, 1 (1994).
[13]W. Blumen, ''Stability of non-planar shear flow of a stratified fluid,'' J. Fluid Mech. **68**, 177 (1975).
[14]J. M. Chomaz, P. Bonneton, and E. J. Hopfinger, ''The structure of the near wake of a sphere moving horizontally in a stratified fluid,'' J. Fluid Mech. **254**, 1 (1993).
[15]G. R. Spedding, F. K. Browand, and A. M. Fincham, ''Turbulence, similarity scaling and vortex geometry in the wake of a towed sphere in a stably stratified fluid,'' J. Fluid Mech. **314**, 53 (1996).
[16]S. I. Voropayev, Xiuzhang Zhang, D. L. Boyer, and H. J. S. Fernando, ''Horizontal jets in a rotating stratified fluid,'' Phys. Fluids **9**, 115 (1997).
[17]R. S. Rogallo, ''Numerical experiments in homogeneous turbulence,'' NASA Tech. Memo. , 81315 (1981).
[18]U. Schumann and T. Gerz, ''Turbulent mixing in stably stratified shear flows,'' J. Appl. Meteorol. **34**, 33 (1995).